ACS APPLIED MATERIALS & INTERFACES

Research Article

www.acsami.org

Energy-Level Engineering at ZnO/Oligophenylene Interfaces with Phosphonate-Based Self-Assembled Monolayers

Melanie Timpel,*[,†] Marco V. Nardi,[†] Giovanni Ligorio,[†] Berthold Wegner,[†] Michael Pätzel,[∥] Björn Kobin,[∥] Stefan Hecht,[∥] and Norbert Koch*[,†,‡]

[†]Institut für Physik & IRIS Adlershof, Humboldt-Universität zu Berlin, Newtonstrasse 15, 12489 Berlin, Germany

[‡]Helmholtz-Zentrum Berlin für Materialien und Energie GmbH, Albert-Einstein-Strasse 16, 12489 Berlin, Germany

[∥]Institut für Chemie, Humboldt-Universität zu Berlin, Brook-Taylor-Strasse 2, 12489 Berlin, Germany

Supporting Information

ABSTRACT: We used aromatic phosphonates with substituted phenyl rings with different molecular dipole moments to form self-assembled monolayers (SAMs) on the Zn-terminated ZnO(0001) surface in order to engineer the energy-level alignment at hybrid inorganic/organic semiconductor interfaces, with an oligophenylene as organic component. The work function of ZnO was tuned over a wide range of more than 1.7 eV by different SAMs. The difference in the morphology and polarity of the SAM-modified ZnO surfaces led to different oligophenylene orientation, which resulted in an orientation-dependent ionization energy that varied by 0.7 eV. The interplay of SAM-induced work function modification and oligophenylene orientation changes allowed tuning of the offsets between the molecular frontier energy levels and the semiconductor band edges over a wide range. Our results demonstrate the versatile use of appropriate SAMs to tune the energy levels of ZnO-based hybrid semiconductor heterojunctions, which is important to optimize its function, e.g., targeting either interfacial energy- or charge-transfer.

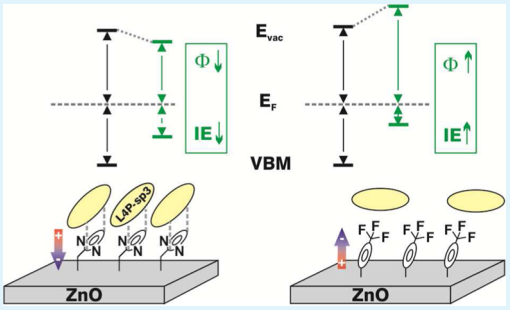

KEYWORDS: *self-assembled monolayer, phosphonic acid, ZnO, energy-level tuning, layered hybrid systems, photoelectron spectroscopy*

1. INTRODUCTION

Engineering the energy-level alignment between inorganic and organic semiconductors is a key step for optimizing (opto-) electronic properties and device performance of hybrid heterojunctions, e.g., for energy-transfer or charge-injection at the inorganic/organic interface. The parameters of interest for controlling the charge-injection barriers are essentially the work function Φ and the valence band maximum (VBM) of the inorganic semiconductor, and the energy of the highest occupied molecular orbital (HOMO) level and lowest unoccupied molecular orbital (LUMO) level, respectively, of the organic semiconductor.[1−3] In the past few decades, alignment of these energy levels relative to each other has commonly been estimated by considering inorganic/organic semiconductor pairs with their individual energy spectrum, i.e., using separately determined values for the work function Φ of the inorganic material as well as the ionization energy (IE) and electron affinity (EA) of the organic material (vacuum level alignment). However, an accurate prediction of the energy-level alignment is hampered by the fact that the material parameters IE and EA of the individual molecule cannot be used as references, since these quantities are substantially affected by specific physicochemical interfacial phenomena, such as intermolecular and molecule−substrate interactions occurring at such hybrid interfaces.[4−6] Therefore, every specific material combination for a layered hybrid system has to be carefully investigated, and the above-mentioned interactions have to be elucidated.

Our approach of energy-level engineering is based on tailoring the ZnO work function via wet-chemical deposition of self-assembled monolayers (SAMs)[7−14] comprising aromatic phosphonates with varying molecular dipole moments; the energy levels of a subsequently deposited organic semiconductor are then realigned to the modified work function. The SAM molecules used here consist of a phosphonic acid (PA) anchoring group and a (pyrimidin-2-yl) methyl (PyPA), a phenyl (PhPA), and a p-trifluoromethylphenyl (pCF_3PhPA) substituent (for chemical structures see Figure 1), i.e., a conjugated moiety with different linkage to the PA anchoring group and varying molecular dipole moment, which allowed changing the work function Φ of ZnO between 2.95 and 4.85 eV. Next, an overlayer consisting of the vacuum-processable ladder-type oligophenylene (L4P-sp3, for chemical structure see Figure 1) was formed by vacuum sublimation and the energy-level alignment studied as a function of the initial SAM-modified ZnO work function. L4P-sp3 was chosen as it was optimized with respect to energy-transfer with ZnO, featuring narrow transitions with high

Received: February 22, 2015
Accepted: May 19, 2015
Published: May 19, 2015

DOI: 10.1021/acsami.5b01669
ACS Appl. Mater. Interfaces 2015, 7, 11900−11907

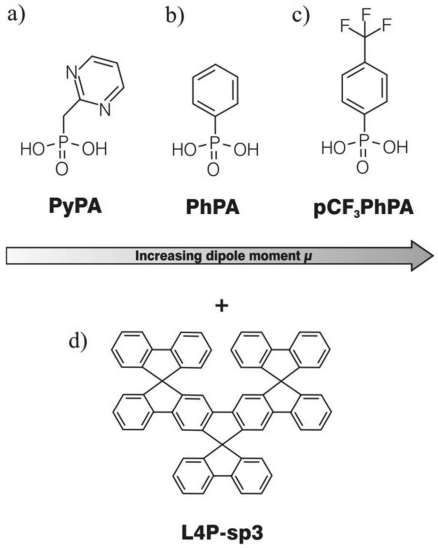

Figure 1. (a–c) Molecular structure of the phosphonic acids used for modification of the ZnO surfaces: (a) (pyrimidin-2-yl) methyl-phosphonic acid (PyPA), (b) phenyl-phosphonic acid (PhPA), (c) p-(trifluoromethyl)phenyl-phosphonic acid (pCF_3PhPA). (d) Structure of the spiro-bridged ladder-type quarterphenyl (L4P-sp3), which was deposited as thin overlayer onto the SAM-modified ZnO surfaces.

oscillator strength in lowest energy transition, small emission–absorption Stokes shift, and an optical gap that corresponds well with that of ZnO.[15−20]

The layered hybrid systems were investigated with synchrotron-based photoelectron spectroscopy (PES): the binding scheme of the phosphonates to ZnO was examined by X-ray photoemission spectroscopy (XPS) and detailed O 1s core level analysis, whereas the energy-level alignment was characterized by ultraviolet photoemission spectroscopy (UPS). With the comprehensive characterization we rationalize the observed work function changes and the overlayer electronic structure on the SAM-modified ZnO surfaces, which will aid the future design of improved molecules for SAM-modification of inorganic/organic semiconductor interfaces.

2. MATERIALS AND METHODS

Single-crystal ZnO(0001)–Zn substrates (CrysTec, Germany) were annealed in a tube furnace (Gero, SR 40–200) under ambient atmosphere at 1000 °C for 2 h (heating rate ∼40 K/min, cooling down ∼3 h) to obtain extended and atomically flat crystal terraces.[13,21] Initially, the ZnO substrates were placed in a quartz glass combustion vessel covered by a planar ZnO sputtering target (99.99% purity). However, the surfaces annealed with sputtering target were less flat compared to the surfaces annealed without sputtering target, as measured by atomic force microscopy;[13] consequently, the samples employed in this study were annealed without a covering ZnO sputtering target. The Zn 2p/O 1s ratio (calculated from our surface-sensitive XPS measurements) of the annealed ZnO surfaces resulted in a value of ∼1, indicating the presence of stoichiometric surfaces.

Figure 1 shows the molecular structure of the aromatic PAs used for surface modification (Figure 1a–c), as well as the oligophenylene consisting of a three spiro-bridged ladder-type quarterphenyl (L4P-sp3, see Figure 1d), which was subsequently deposited as overlayer. (Pyrimidin-2-yl) methyl-phosphonic acid (PyPA, see Figure 1 a) was synthesized as described by Lange et al.[14] and has a methylene group (alkyl spacer) between the PA anchoring group and the pyrimidine phenyl ring. Phenyl-phosphonic acid (PhPA, see Figure 1b) and p-(trifluoromethyl)phenyl-phosphonic acid (pCF_3PhPA, see Figure 1c) were obtained from Aculon, Inc. and used as received. In the latter two cases, the substituted phenyl ring is directly linked to the PA anchoring group.

Well-ordered and uniform SAMs on ZnO were prepared via three preparation cycles,[13] each of which consists of the following steps: (a) immersion of the substrates in a 1 mM tetrahydrofuran (THF, anhydrous) solution of the corresponding PA for 2 h; (b) annealing on a hot plate under ambient atmosphere at 140 °C for 1/2 h; (c) sonication in THF for 20 min.

Improved lateral homogeneity of the SAMs due to the three applied cycles of immersion, annealing, and sonication was previously confirmed by XPS core level spectra,[13] which were recorded at different positions across the SAM-modified sample surface.

L4P-sp3 was sublimed under UHV conditions from a resistively heated quartz crucible. The molecular flux was monitored with a quartz crystal microbalance and was set to a deposition rate equivalent to a nominal 1 Å film mass-thickness per minute, using a density of 1.6 g/cm^3 and assuming the same sticking coefficient on the Au-coated quartz of the microbalance and the (unmodified and SAM-modified) ZnO surfaces.

Photoemission studies were performed at the PM4 beamline, SurICat experimental station, of the BESSY II synchrotron radiation facility (Berlin, Germany) with a base pressure of 2×10^{-10} mbar. Photoemission data were recorded using a Scienta SES 100 hemispherical electron energy analyzer with an energy resolution of 120 meV in normal emission geometry. A photon energy of 35 eV was selected for the secondary electron cutoff (SECO) and valence energy region UPS spectra. For the determination of the work function, the SECO spectra were measured with the sample biased at −10 V to clear the analyzer work function.

Photon energies of 244, 385, 505, 636, and 844 eV were used for the Zn 3s and P 2p, C 1s, N 1s, O 1s, and F 1s core levels, respectively. In this way, the kinetic energy of the emitted photoelectrons was kept at ∼100 eV for each chemical species to probe similar sample depths with high surface sensitivity. Photon fluxes were minimized by inserting a metal filter in the beam path to avoid possible radiation damage of the molecules during beam exposure[13] and to avoid surface photovoltage shifts.[22,23] To investigate the stability of the phosphonate molecules, the C 1s, F 1s/N 1 s, as well as Zn 3s and P 2p core level regions of each SAM-modified ZnO surface were carefully checked (see Figures S1 and S2, Supporting Information). Since the Zn 3s peak is very close to the P 2p peak (∼7 eV different binding energy), the Zn 3s and P 2p region was additionally recorded at 844 (i.e., kinetic energy of 700 eV). This allowed us to investigate depth-dependent trends and to identify possible effects due to surface band bending (in ZnO). The XPS core level fitting was performed by Voigt line shape deconvolution after the background subtraction of a Shirley function.

3. RESULTS

3.1. Binding of Phosphonates to ZnO. The ability to reliably tune the work function of the ZnO surface with phosphonate SAMs and to have stable interfaces requires substantiation by a detailed characterization of their binding to ZnO. Similar to our previous study,[13] the binding modes of the phosphonate anchoring group to the ZnO surface were elucidated by a thorough analysis of the O 1s core level and its chemical components before and after surface modification (see Figure 2). The annealed (unmodified) ZnO surface (Figure 2a) exhibits a main peak at 531.2 eV binding energy (BE) stemming from bulk oxygen as well as a high BE shoulder at 532.6 eV stemming mainly from surface hydroxyl (−OH) groups.[24] These findings are in good agreement with our previously obtained results for the unmodified ZnO surface, which was annealed under similar conditions.[13]

After surface modification (Figure 2b–d), the two initial components (bulk oxygen and surface–OH) are markedly decreased. Furthermore, the O 1s spectrum of each SAM-modified ZnO surface can be fitted with three additional

DOI: 10.1021/acsami.5b01669
ACS Appl. Mater. Interfaces 2015, 7, 11900–11907

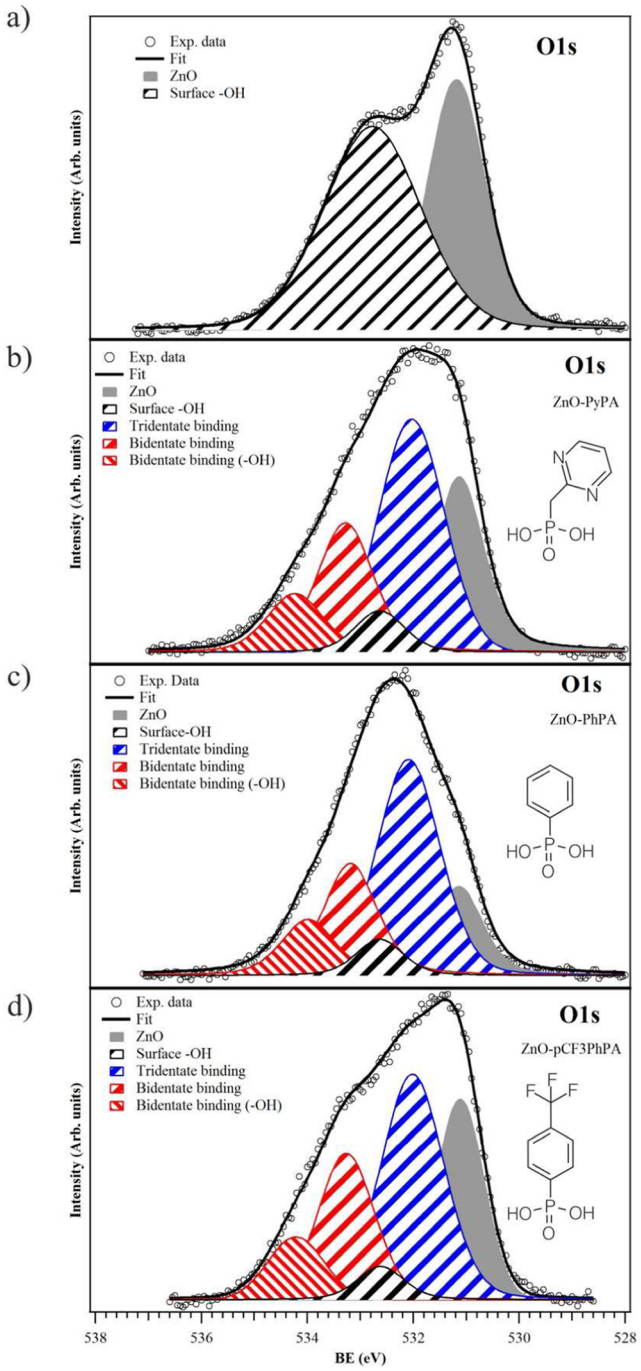

Figure 2. O 1s core level spectra (background subtracted) of the (a) unmodified and (b) PyPA-, (c) PhPA-, and (d) pCF_3PhPA-modified ZnO surface.

components, which were previously assigned on the basis of their binding energy shifts (with respect to the bulk oxygen) to two different PA binding modes,[13,25] i.e., bidentate and tridentate binding (red and blue components in Figure 2b–d). Table 1 summarizes the binding energies of the O 1s core levels for the three SAM-modified ZnO surfaces.

As previously found for the pCF_3PhPA-modified ZnO surface,[13] PyPA and PhPA also adsorb on ZnO via a mixture of bidentate and tridentate binding configurations (Figure 2b,c). Furthermore, the O 1s core level analysis of the pCF_3PhPA-modified ZnO surface in Figure 2d confirms our previous findings.[13] The fraction of bidentate to tridentate binding is

Table 1. Binding Energy and Full Width at Half Maximum (FWHM) of the Surface Components As Calculated from O 1s Core Level Analysis of the SAM-Modified ZnO Surfaces (Spectra in Figure 2)

	binding energy (eV)				
sample	ZnO	surface −OH	tridentate binding	bidentate binding	bidentate binding (−OH)
ZnO + PhPA	531.1	532.6	532.0	533.3	534.2
ZnO + pCF_3PhPA	531.1	532.6	532.0	533.3	534.2
ZnO + PyPA	531.1	532.6	532.0	533.3	534.2

similar in all three cases. Assuming the same number of binding sites theoretically available on the ZnO surface,[13] a similar fraction of bidentate to tridentate binding in the present study points to a similar surface coverage on ZnO for the three aromatic phosphonates (i.e., on the order of 4 molecules/nm^2, as discussed in ref 13). However, a slightly higher coverage for PhPA is indicated by the higher attenuation of the ZnO related feature in XPS in Figure 2c.

3.2. Electronic Structure of L4P-sp3/PA-Modified ZnO Interfaces. In the present study, each individual ZnO surface was initially characterized before surface modification (black curves in Figures 3–5). The work function Φ of the unmodified ZnO surface (derived from the SECO) was found to be in the range Φ = 3.65–3.80 eV. In the following, changes of the work function $\Delta\Phi$ after surface modification are referred to the corresponding pristine ZnO surface. The onsets of the valence band maximum (VBM) of the unmodified/SAM-modified ZnO surfaces, and the HOMO level of L4P-sp3, respectively, are found by linear extrapolation of the leading edge to zero intensity (see black arrows in Figures 3d–5d). The BE of the VBM for unmodified ZnO surfaces was in the range 3.25–3.35 eV. For comparison, the data shown as dashed gray lines in Figures 3–5 correspond to a nominal coverage of 50 Å (thick layer) L4P-sp3 deposited onto an unmodified ZnO surface; this thick layer of L4P-sp3 serves as a reference for the work function ($\Phi_{L4P\text{-}sp3}$ = 3.60 eV) and the typical valence structure of a L4P-sp3 bulk material (with the onset of the HOMO at 2.05 eV BE).

As can be seen for the PyPA-modified ZnO surface (red line in Figure 3a), the work function is lowered by $\Delta\Phi$ = −0.7 eV relative to the unmodified ZnO surface. After deposition of nominal coverage of 5 Å L4P-sp3 (blue line in Figure 3a), the work function increases (by 0.4 eV), and remains nearly constant at 3.3 eV throughout further deposition of L4P-sp3 (green and orange lines in Figure 3a). This work function increase is a consequence of Fermi-level pinning at the lowest unoccupied density of states of the L4P-sp3 layer, which leads to electron transfer to the overlayer and thus the Φ increase.[20]

Figure 3b–d shows spectra of the valence region of the unmodified, PyPA-modified, and L4P-sp3/PyPA-modified ZnO surface (with increasing L4P-sp3 coverage), respectively. The extended valence region spectrum of the PyPA-modified ZnO surface (red line in Figure 3b) is characterized by two relatively broad emission bands, which are labeled as A′ and B′ in Figure 3b and are located at 6.45 and 10.60 eV BE, respectively. The valence region UPS spectrum after deposition of a 5 and 12 Å L4P-sp3 overlayer (blue and green line in Figure 3b, respectively) clearly exhibits additional features. For a better insight into the structure of the frontier orbital levels, Figure 3c displays a zoom of the valence region close to the Fermi level E_F. As is obvious by comparison with the valence structure of the

DOI: 10.1021/acsami.5b01669
ACS Appl. Mater. Interfaces 2015, 7, 11900–11907

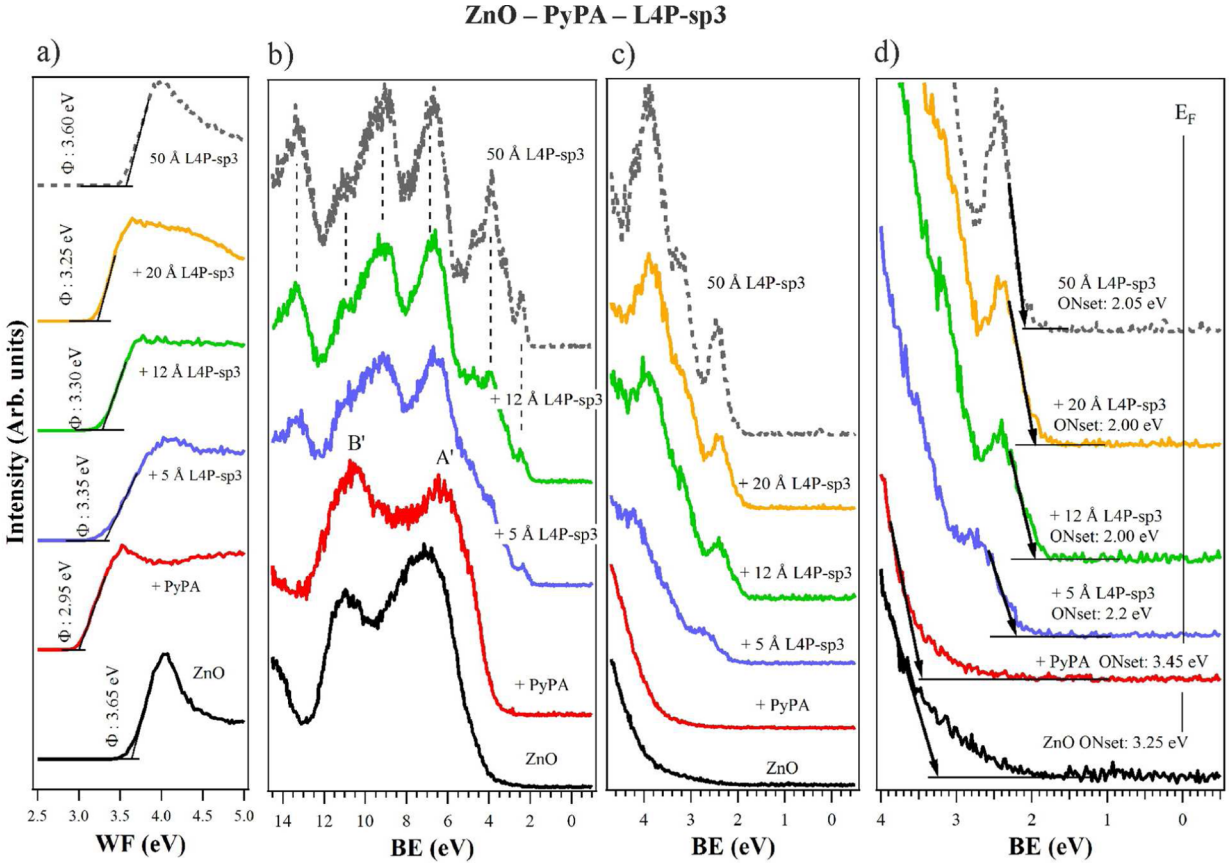

Figure 3. (a) SECO and (b–d) valence band region UPS spectra of the unmodified, PyPA-modified, and L4P-sp3/PyPA-modified ZnO surface (with increasing L4P-sp3 coverage) as indicated in the figure. (b) Extended region of the valence band spectra, and (c, d) subsequent zooms into the near E_F region.

thick L4P-sp3 layer (dashed gray line in Figure 3b–d), those new features can be clearly attributed to the L4P-sp3 molecule. With the subsequent zoom in Figure 3d, it becomes obvious that surface modification shifts the VBM only very slightly (e.g., by +0.2 eV in the case of PyPA modification). After deposition of a 5 Å L4P-sp3 overlayer (blue line in Figure 3d), the onset arising from the HOMO of L4P-sp3 is found at 2.2 eV BE. With increasing deposition of L4P-sp3, the HOMO onset slightly shifts to lower BE (2.00 eV) approaching the value of the bulk material, i.e., 2.05 eV.

In contrast, surface modification of ZnO with PhPA (red line in Figure 4a) shifts the SECO only slightly and yields a similar work function as that of the unmodified substrate ($\Delta\Phi$ = +0.05 eV, Φ = 3.75 eV). After deposition of a 5 and 12 Å L4P-sp3 overlayer, respectively, the work function of the hybrid system (L4P-sp3/PhPA-modified ZnO surface) is constant within 50 meV.

The extended valence region UPS spectrum of the PhPA-modified ZnO surface (red line in Figure 4b) shows a similar intensity ratio between the two features labeled as A and C in Figure 4b as compared to the ratio of the same features before surface modification. In addition, after surface modification a new emission band labeled as B at 9.6 eV BE is clearly visible. Subsequent deposition of a L4P-sp3 overlayer (blue and green line in Figure 4c) gradually changes the valence structure indicating an overlap of residual emission from the PhPA-modified ZnO surface with those from L4P-sp3. After deposition of 12 Å L4P-sp3 (green line in Figure 4b) the valence structure already resembles that of the of the thick L4P-sp3 layer with the HOMO onset at 1.95 eV (green line in Figure 4d).

Different from the PyPA- and PhPA-modified ZnO surfaces, the work function of the pCF_3PhPA-modified ZnO surface (red line in Figure 5a) is significantly increased ($\Delta\Phi$ = +1.05 eV, Φ = 4.85 eV) with respect to the unmodified substrate. The increase of the work function is in good agreement with our previous studies of the pCF_3PhPA-modified ZnO surface.[13] As in the cases before (see Figures 3a and 4a), the work function is not markedly affected by subsequent deposition of a (5 and 12 Å) L4P-sp3 overlayer (blue and green in Figure 5a). Even after deposition of a nominal thickness of 20 Å (orange in Figure 5a), the work function of the L4P-sp3/pCF_3PhPA-modified ZnO surface remains 0.9 eV higher with respect to the unmodified substrate.

Figure 5b–d shows valence spectra of the unmodified, pCF_3PhPA-modified, and L4P-sp3/pCF_3PhPA-modified ZnO surface. Photoemission bands labeled as A–D in Figure 5b are clearly detectable for the pCF_3PhPA modification of ZnO surface. By comparison with our previous density functional theory (DFT) calculations,[13] we could assign these features A–D to a superposition of pCF_3PhPA molecular levels and emission from ZnO. It is noteworthy that, in the case of the pCF_3PhPA-modified ZnO surface, the deposition of L4P-sp3 leads mainly to a "smearing out" of these features A–D, and no clear features characteristic for L4P-sp3 can be identified in Figure 5b. However, in the zoom shown in Figure 5c,d, at least the frontier level structure of L4P-sp3 with the onset of the HOMO at 1.20 eV becomes visible. Here, the value of the HOMO onset BE is

DOI: 10.1021/acsami.5b01669
ACS Appl. Mater. Interfaces 2015, 7, 11900–11907

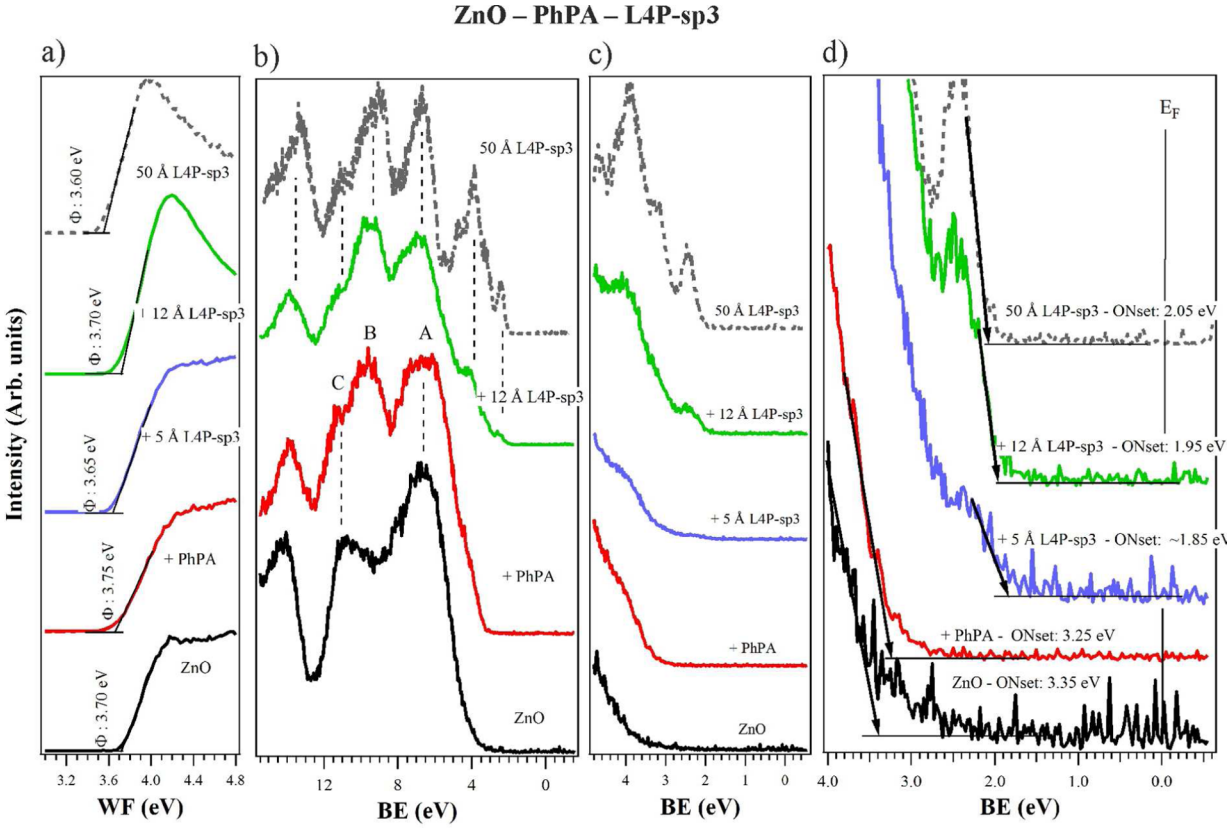

Figure 4. (a) SECO and (b–d) valence band region UPS spectra of the unmodified, PhPA-modified, and L4P-sp3/PhPA-modified ZnO surface (with increasing L4P-sp3 coverage) as indicated in the figure. (b) Extended region of the valence band spectra, and (c, d) subsequent zooms into the near E_F region.

significantly lower than that of the L4P-sp3 bulk material (BE = 2.05 eV).

4. DISCUSSION

After surface modification, both the VBM position for the SAM-modified ZnO surface and shifts of ZnO-derived core levels must be accounted for to differentiate between the contribution of changed (surface) band bending within ZnO to the total work function change $\Delta\Phi$ and that of the phosphonates' dipole. As can be seen in Figures S2 and S3 (Supporting Information), the Zn 3s peak of all SAM-modified ZnO surfaces, and the pristine one, was constant at ∼140 eV BE, independent of the photon energy used in the present study (i.e., 244 and 844 eV). Therefore, any change in ZnO band bending by surface modification is negligible, i.e., $\Delta\Phi$ only results from the molecular dipoles induced by the adsorption of the phosphonates onto the ZnO surfaces. Previous studies also report only very small changes in band bending (<100 meV) for phenyl-phosphonates on ZnO,[26] and no band bending in p-sexiphenyl (6P)/ZnO(0001) hybrid structures.[6] Figure 6a–c schematically shows the interfacial energy-level diagrams of the unmodified and the corresponding SAM-modified ZnO surfaces, as well as the L4P-sp3/SAM-modified ZnO hybrid structures, as derived from our UPS measurements. In addition, Figure 6d displays the bulk electronic properties of L4P-sp3 (50 Å thick layer on unmodified ZnO surface). The ionization energy IE of the bare L4P-sp3 molecule, measured as the difference between the HOMO onset and the vacuum level E_{vac}, amounts to 5.65 eV.

In the present study, the work function change induced by SAM surface modification ranges from $\Delta\Phi$ = −0.7 eV (PyPA-modified ZnO) to $\Delta\Phi$ = +1.05 eV (pCF_3PhPA-modified ZnO). This range of work function change is comparable with previous reports[14] using related phosphonates on ZnO(0001)−Zn and ZnO(000$\bar{1}$)−O single crystals. In a first approximation, the change in the work function can be related to the direction and magnitude of the molecular dipole moment μ of the corresponding aromatic phosphonate.[13,14,25,27] The adsorption of PyPA (μ < 0; negative sign indicates that the dipole of the adsorbed molecule points toward the surface) lowers the work function of ZnO, whereas the adsorption of PhPA ($\mu \geq 0$) keeps it approximately constant, and pCF_3PhPA ($\mu \gg 0$) increases it.

After deposition of a 12 Å L4P-sp3 overlayer onto the PyPA- and PhPA-modified ZnO surface, both valence spectra show the characteristic features of L4P-sp3 (see Figures 3b and 4b). In contrast to that, no appreciable change in the valence structure is observed for the same nominal thickness (i.e., 12 Å) L4P-sp3 deposited onto the pCF_3PhPA-modified ZnO surface (see Figure 5b). Since pCF_3PhPA molecules adopt an approximately upright-standing orientation on ZnO(0001),[13] this difference can be explained by a lower sticking of the L4P-sp3 molecules on the partially fluorinated pCF_3PhPA-modified ZnO surface (i.e., "Teflon-like" behavior), as compared to the (nonpolar) PhPA- and PyPA-modified ZnO surfaces. Therefore, for the same nominal L4P-sp3 thickness, it is expected that the pCF_3PhPA-modified ZnO surface is only partially covered by L4P-sp3 islands (i.e., valence spectrum mainly resembles that of pCF_3PhPA), whereas both the PyPA- and the PhPA-modified ZnO surface are completely covered by L4P-sp3 (i.e., valence spectrum resembles that of L4P-sp3).

DOI: 10.1021/acsami.5b01669
ACS Appl. Mater. Interfaces 2015, 7, 11900−11907

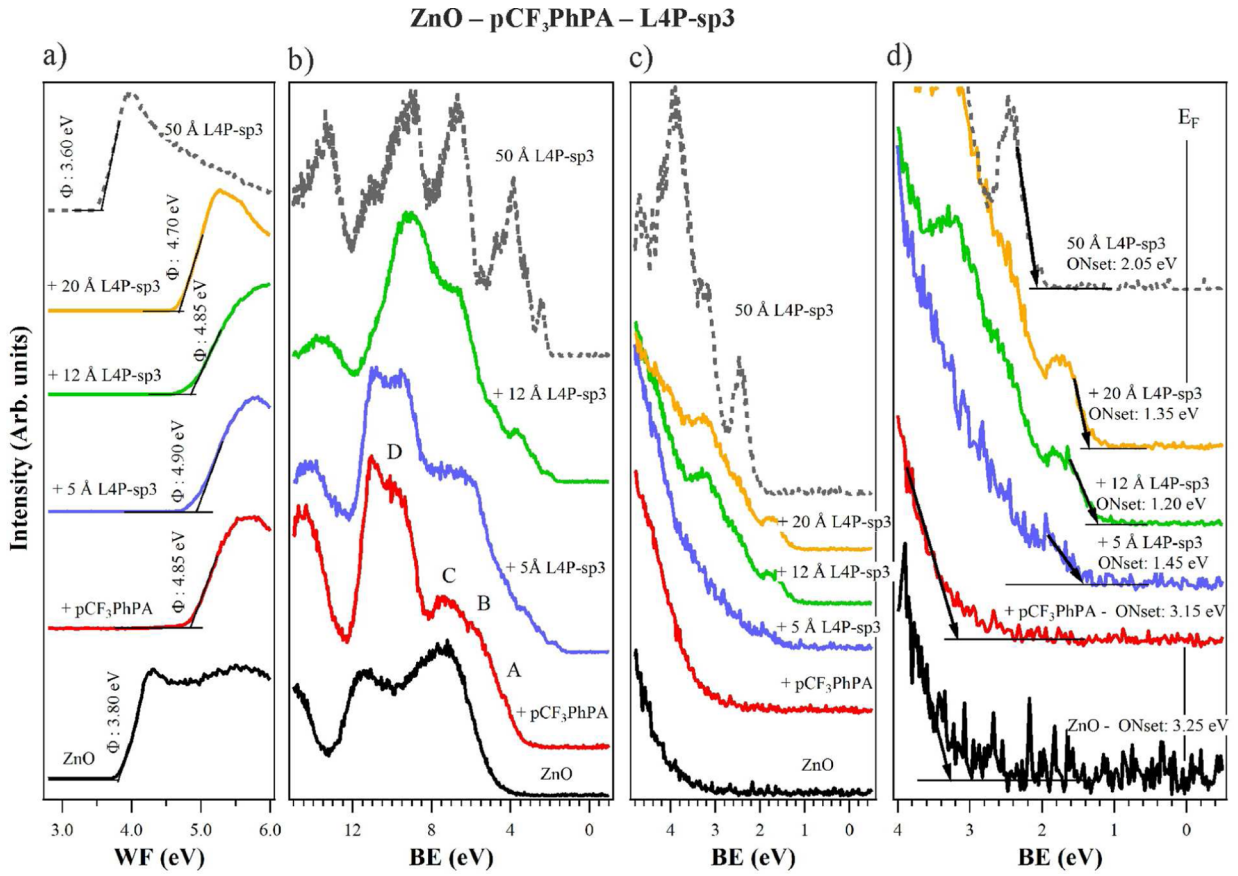

Figure 5. (a) SECO and (b–d) valence band region UPS spectra of the unmodified, pCF_3PhPA-modified, and L4P-sp3/pCF_3PA-modified ZnO surface (with increasing L4P-sp3 coverage) as indicated in the figure. (b) Extended region of the valence band spectra, and (c, d) subsequent zooms into the near E_F region.

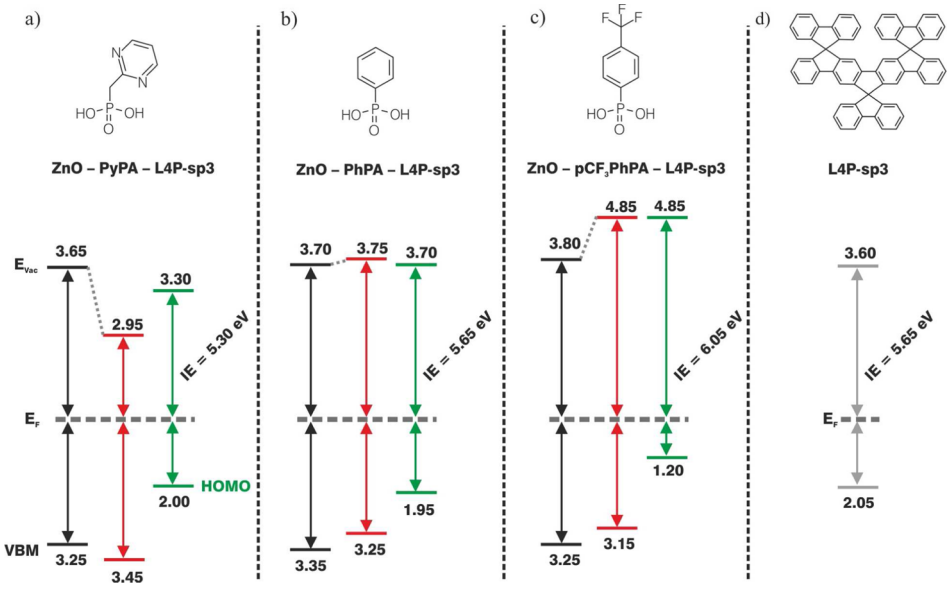

Figure 6. Energy-level diagrams of the unmodified ZnO surfaces (black), the corresponding PA-modified ZnO surfaces (red), and (a nominal thickness of 12 Å) L4P-sp3 deposited on the (a) PyPA-, (b) PhPA-, and (c) pCF_3PhPA-modified ZnO surface (green). (d) Ionization energy IE of the L4P-sp3 molecule (50 Å thick layer on unmodified ZnO).

A further prominent finding is that the ionization energy IE of L4P-sp3 on the PyPA-modified ZnO (see Figure 6a) is 0.35 eV lower compared to the thick-film L4P-sp3 sample (see Figure 6d), whereas IE of L4P-sp3 on pCF_3PhPA-modified ZnO (see Figure 6c) is 0.4 eV higher. This is an indication for different molecule–substrate interactions between the L4P-sp3 overlayer with the underlying SAM-modified ZnO surface, since different molecular aggregation/morphology can lead to different offsets

DOI: 10.1021/acsami.5b01669
ACS Appl. Mater. Interfaces 2015, 7, 11900–11907

between the molecular frontier levels and those of the substrate.[6,28] On the basis of previous findings,[6,28] different molecular orientation can result in different IE values (of more than 0.5 eV) because of collective electrostatic effects. In the case of the L4P-sp3/pCF_3PhPA-modified ZnO hybrid system, due to the extremely low affinity of most organic compounds toward fluoropolymer ("Teflon-like") surfaces,[29] it is reasonable to assume a "flat-lying" orientation (i.e., molecules adsorb with their molecular plane shown in Figure 1d parallel to the substrate surface) of the L4P-sp3 on top of the pCF_3PhPA-modified ZnO surface. This assumption (i.e., flat-lying arrangement) is corroborated by the higher IE value (by 0.4 eV) compared to that of the bulk L4P-sp3, in agreement with an increased IE and flat-lying adsorption geometry as previously found for p-sexiphenyl (6P) on ZnO(0001).[6] In the case of PyPA, the methylene group (alkyl spacer) between the PA anchoring group and the pyrimidine phenyl ring (see Figure 1a) renders the linkage between the binding site and the aromatic moiety more flexible. As a consequence, it has been theoretically[25] and experimentally[14] found that the tilt angle of the phenyl ring is more oblique (43−45°) with respect to the substrate normal. Therefore, owing to relatively strong $\pi-\pi$ interactions between the conjugated orbitals of the PyPA and L4P-sp3 molecules, the L4P-sp3 is forced to adsorb in a more upright-standing/inclined adsorption geometry, as also suggested by the valence spectra comparison shown in Figure S4 (see Supporting Information). The assumption of more upright-standing geometry and the detection of a lower IE value is again in agreement with a decreased IE together with an upright-standing adsorption geometry as previously found for 6P/ZnO($10\bar{1}0$).[6]

5. CONCLUSIONS

In the present work, we demonstrated that aromatic phosphonates with different dipolar substitutions (i) form robust SAMs on ZnO (with bidentate and tridentate binding) and (ii) allow for engineering the work function of ZnO and the energy-level alignment between the inorganic semiconductor ZnO and an organic semiconductor over a wide range of more than 1.7 eV. For all three cases, bare ZnO, PyPA/ZnO, and PhPA/ZnO, the energy difference between the valence band maximum of ZnO and the onset of the L4P-sp3 HOMO is essentially the same (ca. 1.3 eV), despite the fact that Φ of PA/ZnO varied between 2.95 and 3.75 eV. The reason for this is to be sought in the pinning of E_F at the unoccupied levels of the L4P-sp3 films, which is in line with the change of the sample work function upon the organic semiconductor deposition. In contrast, the work function of pCF_3PhPA/ZnO is sufficiently high (4.85 eV) to avoid E_F-pinning at both the occupied and unoccupied levels of the organic semiconductor, so that vacuum level alignment prevails and the energy offset between ZnO valence band maximum and L4P-sp3 HOMO is substantially increased to 1.95 eV. This offset is yet limited by the fact that the average orientation of L4P-sp3 on this, in part, fluorine-terminated surface is such that the ionization energy is higher compared to the other cases presented here. If one could change the molecular orientation such that the ionization energy is lower (as on bare ZnO or PhPA/ZnO), even E_F-pinning at the occupied level could be induced.

A strategy that might allow for achieving controllable molecule−substrate interactions (and thus molecular orientation and tunable energy-level offsets) is therefore highly desirable. The widely tunable work function of ZnO with PA-SAMs in a stable fashion has important implications for the design and performance of electronic devices.

■ ASSOCIATED CONTENT

Supporting Information

C 1s, F 1s/N 1s (Figure S1), as well as Zn 3s and P 2p (Figure S2 and S3) core level spectra, and scaled Valence band region UPS spectra (Figure S4). The Supporting Information is available free of charge on the ACS Publications website at DOI: 10.1021/acsami.5b01669.

■ AUTHOR INFORMATION

Corresponding Authors

*E-mail: mtimpel@physik.hu-berlin.de.
*E-mail: norbert.koch@physik.hu-berlin.de.

Author Contributions

The manuscript was written through contributions of all authors. All authors have given approval to the final version of the manuscript. M.T. and M.V.N. contributed equally.

Notes

The authors declare no competing financial interest.

■ ACKNOWLEDGMENTS

This work was supported by the SFB951 (DFG), the European Commission FP7 Project HYMEC (Grant No. 263073), and the Helmholtz-Energie-Allianz "Hybrid-Photovoltaik".

■ REFERENCES

(1) Ishii, H.; Sugiyama, K.; Ito, E.; Seki, K. Energy Level Alignment and Interfacial Electronic Structures at Organic/Metal and Organic/Organic Interfaces. *Adv. Mater.* **1999**, *11*, 605−625.

(2) Koch, N. Organic Electronic Devices and Their Functional Interfaces. *ChemPhysChem* **2007**, *8*, 1438−1455.

(3) Braun, S.; Salaneck, W. R.; Fahlman, M. Energy-Level Alignment at Organic/Metal and Organic/Organic Interfaces. *Adv. Mater.* **2009**, *21*, 1450−1472.

(4) Hill, I. G.; Rajagopal, A.; Kahn, A.; Hu, Y. Molecular Level Alignment at Organic Semiconductor-Metal Interfaces. *Appl. Phys. Lett.* **1998**, *73*, 662−664.

(5) Ueno, N.; Kera, S. Electron Spectroscopy of Functional Organic Thin Films: Deep Insights into Valence Electronic Structure in Relation to Charge Transport Property. *Prog. Surf. Sci.* **2008**, *83*, 490−557.

(6) Blumstengel, S.; Glowatzki, H.; Sadofev, S.; Koch, N.; Kowarik, S.; Rabe, J. P.; Henneberger, F. Band-Offset Engineering in Organic/inorganic Semiconductor Hybrid Structures. *Phys. Chem. Chem. Phys.* **2010**, *12*, 11642−11646.

(7) Paniagua, S. A.; Hotchkiss, P. J.; Jones, S. C.; Marder, S. R.; Mudalige, A.; Marrikar, F. S.; Pemberton, J. E.; Armstrong, N. R. Phosphonic Acid Modification of Indium-Tin Oxide Electrodes: Combined XPS/UPS/Contact Angle Studies. *J. Phys. Chem. C* **2008**, *112*, 7809−7817.

(8) Jee, S. H.; Kim, S. H.; Ko, J. H.; Kim, D.-J.; Yoon, Y. S. Wet Chemical Surface Modification of ITO by a Self Assembled Monolayer for an Organic Thin Film Transistor. *J. Ceram. Process. Res.* **2008**, *9*, 42−45.

(9) Cheng, X.; Noh, Y.-Y.; Wang, J.; Tello, M.; Frisch, J.; Blum, R.-P.; Vollmer, A.; Rabe, J. P.; Koch, N.; Sirringhaus, H. Controlling Electron and Hole Charge Injection in Ambipolar Organic Field-Effect Transistors by Self-Assembled Monolayers. *Adv. Funct. Mater.* **2009**, *19*, 2407−2415.

(10) Hotchkiss, P. J.; Li, H.; Paramonov, P. B.; Paniagua, S. A.; Jones, S. C.; Armstrong, N. R.; Brédas, J.-L.; Marder, S. R. Modification of the Surface Properties of Indium Tin Oxide with Benzylphosphonic Acids: A Joint Experimental and Theoretical Study. *Adv. Mater.* **2009**, *21*, 4496−4501.

DOI: 10.1021/acsami.5b01669
ACS Appl. Mater. Interfaces 2015, 7, 11900−11907

(11) Sharma, A.; Hotchkiss, P. J.; Marder, S. R.; Kippelen, B. Tailoring the Work Function of Indium Tin Oxide Electrodes in Electrophosphorescent Organic Light-Emitting Diodes. *J. Appl. Phys.* **2009**, *105*, 084507.
(12) Wang, M.; Hill, I. G. Fluorinated Alkyl Phosphonic Acid SAMs Replace PEDOT:PSS in Polymer Semiconductor Devices. *Org. Electron.* **2012**, *13*, 498−505.
(13) Timpel, M.; Nardi, M. V.; Krause, S.; Ligorio, G.; Christodoulou, C.; Pasquali, L.; Giglia, A.; Frisch, J.; Wegner, B.; Moras, P.; Koch, N. Surface Modification of ZnO(0001)−Zn with Phosphonate-Based Self-Assembled Monolayers: Binding Modes, Orientation and Work Function. *Chem. Mater.* **2014**, *26*, 5042−5050.
(14) Lange, I.; Reiter, S.; Pätzel, M.; Zykov, A.; Nefedov, A.; Hildebrandt, J.; Hecht, S.; Kowarik, S.; Wöll, C.; Heimel, G.; Neher, D. Tuning the Work Function of Polar Zinc Oxide Surfaces Using Modified Phosphonic Acid Self-Assembled Monolayers. *Adv. Funct. Mater.* **2014**, *24*, 7014−7024.
(15) Scherf, U.; Müllen, K.; Polyarylenes. and Poly(arylenevinylenes), 7 - A Soluble Ladder Polymer via Bridging of Functionalized Poly(p-Phenylene)-Precursors. *Makromol. Chem., Rapid Commun.* **1991**, *12*, 489−497.
(16) Grimsdale, A. C.; Müllen, K. Oligomers and Polymers Based on Bridged Phenylenes as Electronic Materials. *Macromol. Rapid Commun.* **2007**, *28*, 1676−1702.
(17) Grimsdale, A. C.; Müllen, K. Bridged Polyphenylenes—from Polyfluorenes to Ladder Polymers. *Adv. Polym. Sci.* **2008**, *212*, 1−48.
(18) Kobin, B.; Grubert, L.; Blumstengel, S.; Henneberger, F.; Hecht, S. Vacuum-Processable Ladder-Type Oligophenylenes for Organic−inorganic Hybrid Structures: Synthesis, Optical and Electrochemical Properties upon Increasing Planarization as Well as Thin Film Growth. *J. Mater. Chem.* **2012**, *22*, 4383−4390.
(19) Bianchi, F.; Sadofev, S.; Schlesinger, R.; Kobin, B.; Hecht, S.; Koch, N.; Henneberger, F.; Blumstengel, S. Cascade Energy Transfer versus Charge Separation in Ladder-Type Oligo(p-phenylene)/ZnO Hybrid Structures for Light-Emitting Applications. *Appl. Phys. Lett.* **2014**, *105*, 233301.
(20) Schlesinger, R.; Bianchi, F.; Blumstengel, S.; Christodoulou, C.; Ovsyannikov, R.; Kobin, B.; Moudgil, K.; Barlow, S.; Hecht, S.; Marder, S. R.; Henneberger, F.; Koch, N. Efficient Light Emission from Inorganic/organic Semiconductor Hybrid Structures by Energy Level Tuning. *Nat. Commun.* **2015**, DOI: 10.1038/ncomms7754.
(21) Götzen, J.; Witte, G. Rapid Preparation of Highly Ordered Ultraflat ZnO Surfaces. *Appl. Surf. Sci.* **2012**, *258*, 10144−10147.
(22) Hecht, M. Role of Photocurrent in Low-Temperature Photoemission Studies of Schottky-Barrier Formation. *Phys. Rev. B* **1990**, *41*, 7918−7922.
(23) Mao, D.; Kahn, A.; Marsi, M.; Margaritondo, G. Synchrotron-Radiation-Induced Surface Photovoltage on GaAs Studied by Contact-Potential-Difference Measurements. *Phys. Rev. B* **1990**, *42*, 3228−3230.
(24) Hotchkiss, P. J.; Malicki, M.; Giordano, A. J.; Armstrong, N. R.; Marder, S. R. Characterization of Phosphonic Acid Binding to Zinc Oxide. *J. Mater. Chem.* **2011**, *21*, 3107−3112.
(25) Wood, C.; Li, H.; Winget, P.; Brédas, J.-L. Binding Modes of Fluorinated Benzylphosphonic Acids on the Polar ZnO Surface and Impact on Work Function. *J. Phys. Chem. C* **2012**, *116*, 19125−19133.
(26) Kedem, N.; Blumstengel, S.; Henneberger, F.; Cohen, H.; Hodes, G.; Cahen, D. Morphology-, Synthesis- and Doping-Independent Tuning of ZnO Work Function Using Phenylphosphonates. *Phys. Chem. Chem. Phys.* **2014**, *16*, 8310−8319.
(27) Romaner, L.; Heimel, G.; Ambrosch-Draxl, C.; Zojer, E. The Dielectric Constant of Self-Assembled Monolayers. *Adv. Funct. Mater.* **2008**, *18*, 3999−4006.
(28) Duhm, S.; Heimel, G.; Salzmann, I.; Glowatzki, H.; Johnson, R. L.; Vollmer, A.; Rabe, J. P.; Koch, N. Orientation-Dependent Ionization Energies and Interface Dipoles in Ordered Molecular Assemblies. *Nat. Mater.* **2008**, *7*, 326−332.
(29) Motreff, A.; Belin, C.; Correa da Costa, R.; El Bakkari, M.; Vincent, J.-M. Self-Adaptive Hydrophilic and Coordinating Teflon Surfaces through a Straightforward Physisorption Process. *Chem. Commun.* **2010**, *46*, 6261−6263.

DOI: 10.1021/acsami.5b01669
ACS Appl. Mater. Interfaces 2015, 7, 11900−11907